

# Science *Reprint*

## Coalescence of Single-Walled Carbon Nanotubes

M. Terrones,<sup>1\*</sup> H. Terrones,<sup>1,2†</sup> F. Banhart,<sup>3‡</sup> J.-C. Charlier,<sup>4</sup>  
and P. M. Ajayan<sup>5</sup>

19 May 2000, Volume 288, pp. 1226–1229

could reduce the required DNA amount, together with use of the “breadth-first” search proposed for large SAT problems (6, 24), where our algorithm must be repeated by the number of the clauses, although several clauses can be processed simultaneously. Upon tackling large instances, PCR may introduce serious errors into computation because all sequences may not be amplified with the same efficiency (7). However, a variation in sequence was still retained after our computation including as many as 70 PCR cycles (25). Further study is necessary for unraveling the nature of the possible bias during PCR.

Another drawback with our method is the incompleteness of our understanding of the nature of hairpin molecules. The limit to the available length of hairpin remains to be determined; the available data suggest that an intact double helix of 30 base pairs is stable enough for closing a 2000-base hairpin loop (26–28). Sequence design or experimental conditions that ensure the hairpin formation and thus reduce the error rate also remain as the major issue for our algorithm. On the other hand, “negative” errors (loss of “solution” molecules) were successfully controlled, because the satisfying strings were finally obtained, despite their small population (0.04% of the total molecules) in the initial DNA pool. This approach for molecular computing, described on a theoretical basis (29) and then implied in some previous experiments (1, 3, 30), sheds a new light on the potential of DNA, not restricted to a carrier of information.

References and Notes

1. L. M. Adleman, *Science* **266**, 1021 (1994).
2. R. J. Lipton, *Science* **268**, 542 (1995).
3. Q. Ouyang, P. D. Kaplan, S. Liu, A. Libchaber, *Science* **278**, 446 (1997).
4. N. Morimoto, M. Arita, A. Suyama, in *DNA Based Computers III*, H. Rubin and D. H. Wood, Eds., vol. 48 of *DIMACS Series in Discrete Mathematics and Theoretical Computer Science* (American Mathematical Society, Providence, RI, 1999), pp. 193–206.
5. A. G. Frutos et al., *Nucleic Acids Res.* **25**, 4748 (1997).
6. H. Yoshida and A. Suyama, in *Preliminary Proceedings of the Fifth International Meeting on DNA Based Computers*, E. Winfree and D. K. Gifford, Eds. (American Mathematical Society, Providence, RI, 1999), pp. 9–20.
7. Q. Liu et al., *Nature* **403**, 175 (2000).
8. D. Faulhammer, A. R. Cukras, R. J. Lipton, L. F. Landweber, *Proc. Natl. Acad. Sci. U.S.A.* **97**, 1385 (2000).
9. G. Paun, G. Rozenberg, A. Salomaa, *DNA Computing: New Computing Paradigms* (Springer-Verlag, Berlin, 1998).
10. M. H. Garzon and R. J. Deaton, *IEEE Trans. Evol. Comput.* **3**, 236 (1999).
11. E. Winfree, in *DNA Based Computers*, R. J. Lipton and E. B. Baumvol, Eds., vol. 27 of *DIMACS Series in Discrete Mathematics and Theoretical Computer Science* (American Mathematical Society, Providence, RI, 1996), pp. 199–221.
12. M. Hagiya, *New Generation Comput.* **17**, 131 (1998).
13. J. Reif, in *DNA Based Computers III*, H. Rubin and D. H. Wood, Eds., vol. 48 of *DIMACS Series in Discrete Mathematics and Theoretical Computer Science* (American Mathematical Society, Providence, RI, 1999), pp. 217–254.
14. T. Yokomori, in *Preliminary Proceedings of the Fifth International Meeting on DNA Based Computers*, E.

- Winfree and D. K. Gifford, Eds. (American Mathematical Society, Providence, RI, 1999), pp. 153–167.
15. E. Winfree, X. Yang, N. Seeman, in *DNA Based Computers II*, L. Landweber and E. Baum, Eds., vol. 44 of *DIMACS Series in Discrete Mathematics and Theoretical Computer Science* (American Mathematical Society, Providence, RI, 1999), pp. 191–213.
16. E. Winfree, F. Liu, L. A. Wenzler, N. C. Seeman, *Nature* **394**, 539 (1998).
17. T. H. LaBean, E. Winfree, J. H. Reif, in *Preliminary Proceedings of the Fifth International Meeting on DNA Based Computers*, E. Winfree and D. K. Gifford, Eds. (American Mathematical Society, Providence, RI, 1999), pp. 121–138.
18. K. Sakamoto et al., *Biosystems* **52**, 81 (1999).
19. J. E. Hopcroft and J. D. Ullman, *Introduction to Automata Theory, Languages and Computation* (Addison-Wesley, Reading, MA, 1979).
20. The details of the DNA sequences and experimental manipulations are available at [www.sciencemag.org/feature/data/1046140.shl](http://www.sciencemag.org/feature/data/1046140.shl).
21. The priming of DNA synthesis by digested literal strings probably produced the “recombinant” strings of the full length, which cannot be distinguished from the undigested DNA. By the definition of literal strings, this unusual priming of DNA synthesis does not generate such literal strings that contain any erroneous literal that is absent in the corresponding clauses of the formula. The profile of the band ladder (the band intensity drastically decreased with the DNA length) indicated that the extent of this contamination was negligible for the size of the present instance. However, rigorous estimation may be necessary for larger instances, and molecular biology techniques could cope with this issue; for example, dideoxyribonucleotides can be added to the 3' end of the digested strings so that they cannot prime DNA synthesis. Recombination between the “solution-candidate” molecules during PCR amplification has been reported (8). This is another possible cause of the band ladder, although PCR amplification of pool 0 by itself did not produce any band ladder (Fig. 3B, lane 1).
22. To avoid the loss of DNA, we amplified the product once after 10 cycles of ePCR by the normal PCR protocol. This amplified DNA was then applied to another 10 cycles of ePCR and was finally recovered by PCR with the primers

- pbs1 and pbs2c that have additional bases of the Eco RI and Hind III sites, respectively, at the 5' end. The shift of the bands to the origin of the electrophoresis was due to the use of these longer PCR primers. The band ladder produced after ePCR was caused probably because the purification of the full-length products after the enzymatic digestion was incomplete, and the contamination of the shorter molecules was amplified during ePCR and the succeeding PCR. The recovered full-length DNA was purified and then digested with the restriction enzymes for cloning in an appropriate vector.
23. D. Mitchell, B. Selman, H. Levesque, in *Proceedings of the 10th National Conference on Artificial Intelligence (AAAI-92)*, P. Rosenbloom and P. Szolovits, Eds. (AAAI Press/MIT Press, Cambridge, MA, 1992), pp. 459–465.
24. M. Ogihara and A. Ray, in *DNA Based Computers III*, H. Rubin and D. H. Wood, Eds., vol. 48 of *DIMACS Series in Discrete Mathematics and Theoretical Computer Science* (American Mathematical Society, Providence, RI, 1999), pp. 255–264.
25. K. Sakamoto et al., data not shown.
26. C. R. Cantor and P. R. Schimmel, *Biophysical Chemistry Part III: The Behavior of Biological Macromolecules* (Freeman, San Francisco, 1980).
27. K. J. Breslauer, R. Frank, H. Blocker, L. A. Marky, *Proc. Natl. Acad. Sci. U.S.A.* **83**, 3746 (1986).
28. D. H. Jones and S. C. Winistorfer, *Nucleic Acids Res.* **20**, 595 (1992).
29. C. H. Bennett, *Int. J. Theor. Phys.* **21**, 905 (1982).
30. F. Guarnieri, M. Fliss, C. Bancroft, *Science* **273**, 220 (1996).
31. These additional data came from the 64 sequenced clones picked up from pools 1 through 3 and 9 clones from other prototype computations. These 73 clones include 71 different literal strings.
32. We thank A. Nishikawa for designing the DNA sequences used in the experiments, E. Winfree for the critical reading of the manuscript, and Y. Husimi for valuable discussions on the physicochemical nature of hairpins. This work was supported in part by the Japan Society for the Promotion of Science under the Research for the Future program (JSPS-RFTF 96I00101).

12 October 1999; accepted 3 April 2000

## Coalescence of Single-Walled Carbon Nanotubes

M. Terrones,<sup>1\*</sup> H. Terrones,<sup>1,2†</sup> F. Banhart,<sup>3‡</sup> J.-C. Charlier,<sup>4</sup> P. M. Ajayan<sup>5</sup>

The coalescence of single-walled nanotubes is studied in situ under electron irradiation at high temperature in a transmission electron microscope. The merging process is investigated at the atomic level, using tight-binding molecular dynamics and Monte Carlo simulations. Vacancies induce coalescence via a zipper-like mechanism, imposing a continuous reorganization of atoms on individual tube lattices along adjacent tubes. Other topological defects induce the polymerization of tubes. Coalescence seems to be restricted to tubes with the same chirality, explaining the low frequency of occurrence of this event.

The driving force for coalescence of particles and supramolecular structures is the reduction in surface and strain energy, however high energy barriers may have to be overcome, particularly in the case of supramolecular systems where factors such as bond rigidity and rotation, structural geometry, and atomic mobility play an important role. In this context, mass spectrometric measurements on hot fullerene vapors (1) and microscopy studies (2, 3) have provided some evidence for fullerene coalescence. However, single-walled carbon nanotubes (SWNTs)

are large molecular assemblies consisting of several thousand atoms. Their basic structure is made of seamless cylinders of sp<sup>2</sup>-like C. Recent reports suggest the possibility of coalescence between these massive molecular structures when they are annealed at high temperatures in the presence of H<sub>2</sub> (4, 5).

Here, we show the coalescence of SWNTs by in situ irradiation and heating in a high-resolution transmission electron microscope (HRTEM) and consider in detail the possible

atomistic mechanisms leading to the merger. The experiments were performed at specimen temperatures of 800°C in an atomic-resolution, 1.25-MeV HRTEM (Jeol-ARM 1250 at the Max-Planck-Institut für Metallforschung in Stuttgart) equipped with a Gatan heating stage. By performing tight-binding molecular dynamics and Monte Carlo calculations on adjacently placed tubes, we show that selection rules (based on the chirality of nanotubes and the kind of defect) dictate whether two adjacent tubes will coalesce. Among various defects studied (such as dangling bonds, vacancies, interstitials, Stone-Wales, and 5-7 defects), vacancies play

the most dominant role in directing the coalescence of nanotubes. Other defects can be responsible for connections between nanotubes that promote their polymerization through  $sp^3$  bonding. Such defects have been previously studied under different circumstances in nanotubes and other graphitic structures (6–11).

SWNT bundles were produced with Ni-Y catalysts in a C arc (12). Nanotube coalescence was promoted by electron irradiation and observed instantaneously on various occasions. In some cases, the events occurred faster than the time resolution ( $\sim 0.1$  s) of the real time TV-rate video camera of the electron microscope. In Fig. 1, only two of the several nanotubes present in the bundle coalesced during this observation. We also observed intermediate stages of coalescence. Figure 2 shows a coalescence process within a SWNT bundle, in which the merger of three tubes takes place over a relatively long time period (3 to 10 min). Initially, two of the outer tubules coalesce rapidly into a larger diameter cylinder of nearly double the circumference (four times the cross section; Fig. 2, A and B). Subsequently, this coalesced tube establishes a “link” with another tubule of smaller diameter (Fig. 2C). The link may be due to a metastable polymerization state of the structures. Consequently, this bridge develops in a dumbbell-like configuration (Fig. 2, D and E). Finally, the three coalesced nanotubes result in a metastable morphology (Fig. 2F). Such processes were frequently observed at the edge of a bundle, probably because free space is needed to establish the merger. Also, because of nanotube multidirectional overlapping, which reduces im-

age contrast during observation, it is hard to clearly observe any coalescence taking place in the interior of the bundles.

In earlier reports of nanotube coalescence (4, 5), it was suggested that the H present during annealing attacks the sides of the nanotubes, thus breaking a C-C bond and producing defective sites (vacancies and dangling bonds) that join together locally forming a seamless bridge. The propagation of this bridge would then open up the tube like a zipper (5). In our experiments, there are no gaseous species present; alternatively, electron irradiation produces vacancies in the network that are responsible for promoting tube coalescence.

We performed tight-binding molecular dynamics (TBMD) calculations to investigate the structural stability and dynamical behavior during nanotube coalescence. TBMD is not as accurate as ab initio calculations; however, it allows the treatment of larger systems with a reduced computational effort and takes into account the essential physicochemical considerations of covalent C-C bonds, thus satisfactorily describing  $sp$ ,  $sp^2$ , and  $sp^3$  hybridization states. We have used TBMD approaches involving an energy functional and a parametrization that previously proved to be successful in the modeling of different allotropes of C and other C-based systems (13, 14).

In the TBMD calculations, two adjacent (10,10) nanotubes containing random vacancies and dangling bonds along the nearest-neighbor edge coalesced into a unique single-walled tube at 1000°C (Fig. 3). The simulation starts with the creation of 20 vacancies in

<sup>1</sup>Instituto de Física, UNAM, Laboratorio Juriquilla, Apartado Postal 1-1010, 76000 Querétaro, Qro., México. <sup>2</sup>School of Chemistry, Physics and Environmental Science, University of Sussex, Brighton BN1 9QJ, UK. <sup>3</sup>Max-Planck-Institut für Metallforschung, Heisenbergstrasse 1, 70569 Stuttgart, Germany. <sup>4</sup>Université Catholique de Louvain, Unité de Physico-Chimie et de Physique des Matériaux, Place Croix du Sud 1, B-1348 Louvain-la-Neuve, Belgium. <sup>5</sup>Department of Materials Science and Engineering, Rensselaer Polytechnic Institute, Troy, NY 12180–3590, USA.

\*Present address: Max-Planck-Institut für Metallforschung, Seestrasse 92, 70174 Stuttgart, Germany.

†To whom correspondence should be addressed. E-mail: terrones@fenix.ifisicacu.unam.mx

‡Present address: Sektion Elektronenmikroskopie, Universität Ulm, 89069 Ulm, Germany.

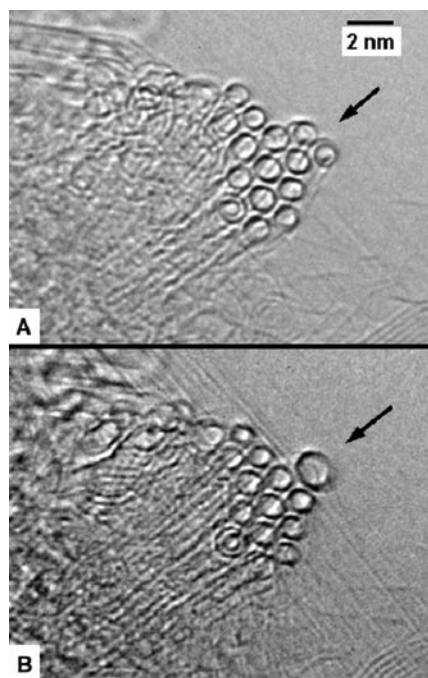


**Fig. 1.** HRTEM images of a SWNT rope cross section, consisting of  $\sim 15$  nanotubes. The cross sections of the tubes are seen where the tube axis is aligned along the viewing direction (direction of the electron beam). (A) Starting bundle and (B) bundle after a few seconds of high-intensity electron irradiation (1.25 MeV) at 800°C. In (B), two of the outer tubes (each approximately 1.1 to 1.2 nm diameter) have coalesced into a larger one of  $\sim 1.8$  to 2.0 nm diameter.

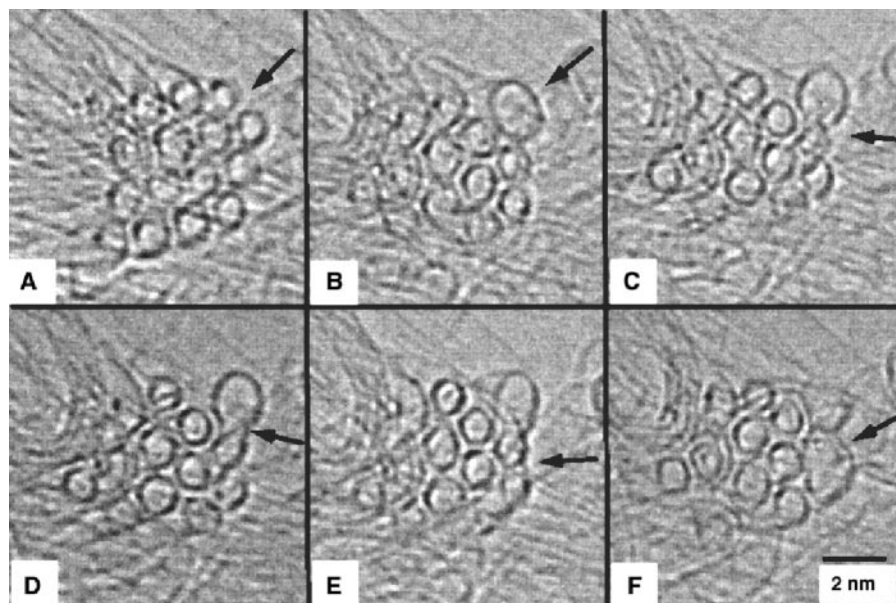


**Fig. 2.** HRTEM images of the coalescence process observed within a bundle of SWNTs. (A) cross sections of 14 nanotubes are clearly observed. (B) Arrow indicates that two of the outer nanotubes coalesced. (C) The larger diameter coalesced tube establishes a link with another nanotube, possibly due to polymerization-like effects, and a second coalescence process is initiated. (D and E) This bridge or link now develops in a “belt” dumbbell-like fashion. (F) The three tubes coalesce into a more circular cross section and the system reaches a metastable state.

two adjacent nanotubes (contained in a 820-atom unit cell) so that coalescence is stimulated (Fig. 3A). In this case, the number of vacancies is only about 2.5% of defects within the cell and can be easily created in our irradiation experiments. In order to obtain optimal integration of equations of motion and energy conservation, TBMD calculations were performed with time steps of 0.7 fs within a total simulation time of 150 ps. The two adjacent tubes were heated to 1000°C so that the creation of tube interconnections on their surface is accelerated. After 100 ps, a connection between the two tubes was established (Fig. 3B), and a zipper-like mechanism proceeded to anneal the structures. Figure 3C reveals that the tubes coalesced after 150 ps into a larger tubule of about 2.6 nm diameter. The coalesced tube still exhibited a few remaining dangling bonds. However, the small number of two-coordinated and four-coordinated atoms demonstrate the stability of nearly pure  $sp^2$  hexagonal framework (Fig. 3C). Unfortunately, the time scale of our simulation prevented us from further studying the development of these vacancies. Additional TBMD calculations (with similar simulation conditions as above) performed on highly defective armchair tube systems containing a large number of vacancies [e.g., a complete row of hexagons extracted from each (10,10) tube within the neighboring region] led to an accelerated coalescence process. However, this model is not as realistic as that involving only 20 vacancies within the cell.

In our experiments, electron irradiation removes C atoms from their lattice sites in the nanotube by knock-on displacements (15–17). Under the conditions of the present experiment, each C atom is displaced approximately every 100 s. The atoms can either be ejected from the tube or migrate as interstitials along the inner or outer surface. The high specimen temperature in this experiment ensures a high mobility of interstitials and hence rapid annealing of defects. The process of radiation damage and annealing kinetics in C nanostructures is described in detail in (16). Because of the dangling bonds associated with the radiation-induced vacancies, the C system will become energetically unstable. If the irradiated tube is isolated, it will shrink by mending these holes through atomic rearrangements, leading to surface reconstruction and dimensional changes (15). On the other hand, when assembled in bundles, the irradiated tube(s) will establish links in order to satisfy most of the dangling bonds. This coalescence phenomenon is also driven by strain energy minimization so that stable tubules of larger diameter are created (18). Our TBMD simulations confirm that coalescence is catalyzed by the presence of dangling bonds and follows a “zipping” process (Fig. 3).

Simulated annealing with the Monte Carlo (MC) method (19) using the many-body Ter-

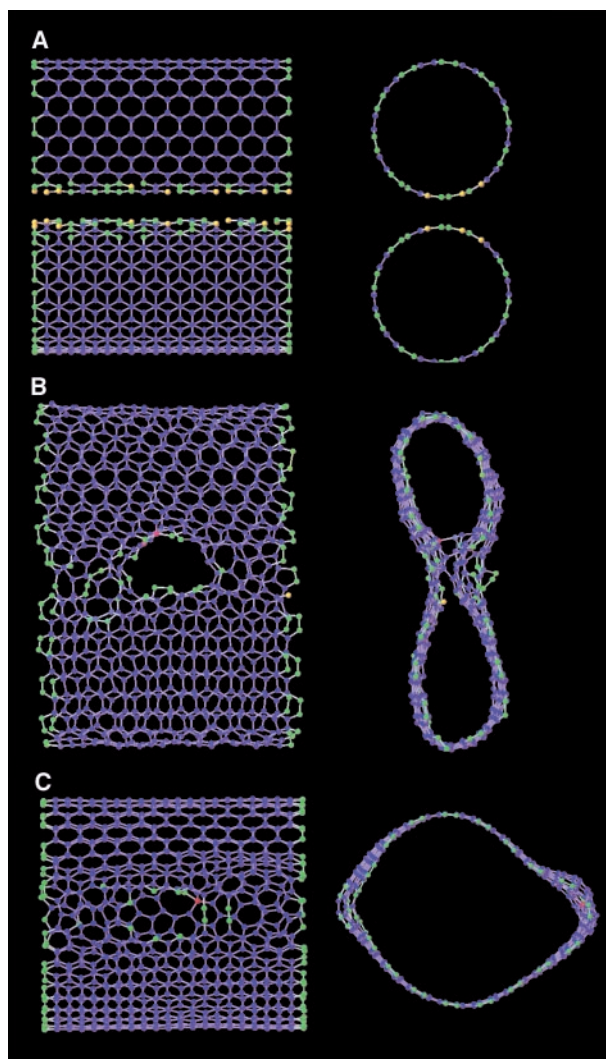


**Fig. 3.** Sequences of coalescence [side (left) and sectional (right) views] between two adjacent (10,10) carbon nanotubes (diameter: 1.36 nm) into a unique single-walled tube of larger diameter. (A) The simulation starts with the creation of 20 vacancies in the lattices of the two tubes (about 2.5% of defects within the cell) in a localized neighboring region, in order to promote coalescence. The unit cell contains 820 C atoms (yellow, green, blue, and red spheres, illustrating an atomic coordination of 1, 2, 3, and 4, respectively). Periodic boundary conditions are imposed along the nanotube axis. TBMD calculations were performed using a time step of 0.7 fs, to assure optimal integration of equations of motion and energy conservation, and for a total simulation time of 150 ps. The two nanotubes were gradually heated to 1000°C in order to accelerate the creation of interlinks and the surface reconstruction. (B) After 100 ps, the connection between the two C networks has been formed and the “zipping” mechanism is proceeding. (C) After 150 ps, the coalescence is completed. The C system is now a cylinder with a diameter of about 2.6 nm. The reconstructed surface after coalescence contains a small number of remaining defects: two-coordinate (12 green spheres) and four-coordinate (1 red sphere).

soff potential, which accurately reproduces cohesive energies and elastic properties of graphite and diamond (20), confirmed that two adjacent (10,10) tubes (480-atom unit cell) containing 20 random vacancies coalesce in temperatures between 1000° and 800°C. The same result is obtained when two (17,0) zig-zag nanotubes (476-atom unit cell), each of them close in diameter to the (10,10) armchair tube, are simulated under similar conditions.

The simulated annealing relaxation (MC) is carried out by slowly decreasing the temperature in 1°C steps starting at 1000°C. Each temperature step is divided into 20 cycles. In each cycle, one atom in the unit cell is chosen and displaced randomly, calculating the energy using the Tersoff potential (20) (periodic boundary conditions are used). This procedure is repeated  $5 \times 10^4$  times within the cycle in order to allow movements of all the atoms in the system (for large runs, e.g., 1000° to  $-273^\circ\text{C}$ ,  $2.5 \times 10^4$  movements per cycle are used). Therefore, at each temperature,  $1 \times 10^6$  atomic movements are carried out ( $1 \times 10^6$  different configurations). When an atom is displaced, the new

configuration is accepted automatically if the total energy of the system decreases; if not, the configuration can be either accepted or rejected according to the Boltzmann factor  $\exp(\Delta E/k_B T)$  using the Metropolis Algorithm (19) (where  $\Delta E$  is the energy difference,  $k_B$  is the Boltzmann constant, and  $T$  is the temperature in K). Subsequently, the final atomic arrangement obtained after the 20th cycle is used as the starting configuration for the next lower temperature iteration. It is found that 20 cycles are optimum in our systems (with  $<500$  atoms in the unit cell). By increasing the number of cycles ( $>20$ ), the computing time increases without improving the resulting outcome. The Tersoff/MC approach has been used before in C systems to investigate nanotube growth (21), the stability of  $C_{20}$  isomers, and the inversion of corannulene ( $C_{20}H_{10}$ ) (22).

MC simulations also reveal that other topological defects lead to vacancies, which will subsequently result in coalescence. In this context, the presence of bond rotational transformations known as Stone-Wales defects (SWDs), where four hexagons are converted

REPORTS

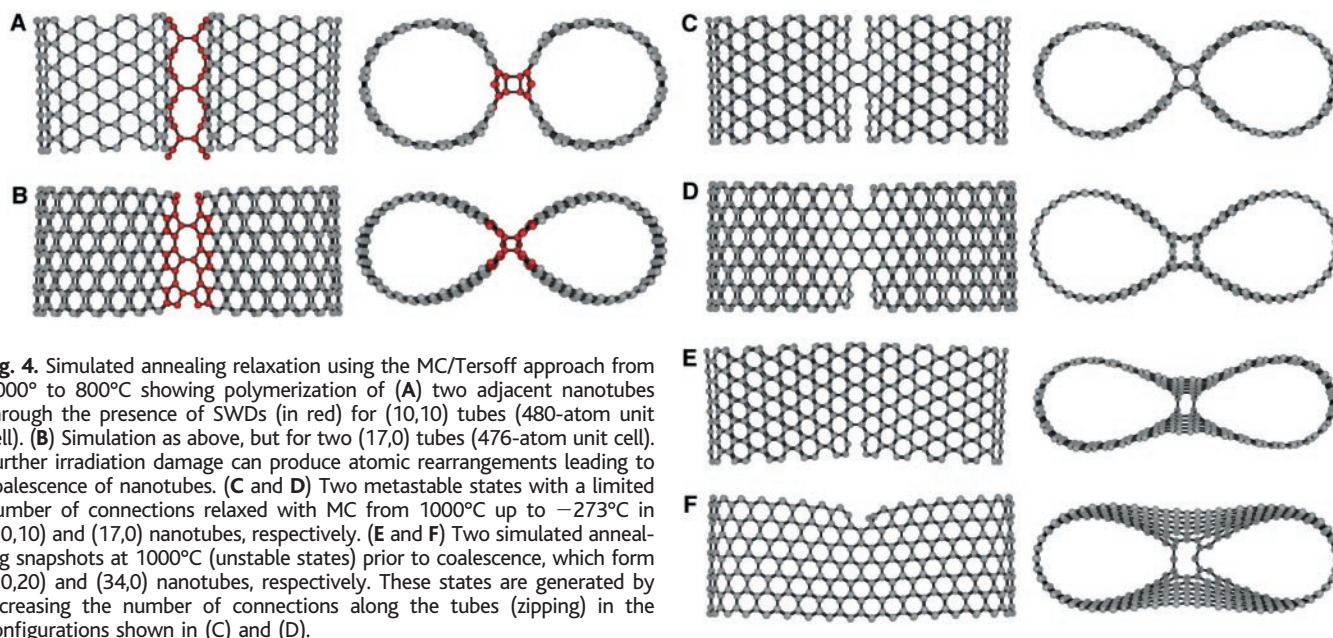


**Fig. 4.** Simulated annealing relaxation using the MC/Tersoff approach from 1000° to 800°C showing polymerization of (A) two adjacent nanotubes through the presence of SWDs (in red) for (10,10) tubes (480-atom unit cell). (B) Simulation as above, but for two (17,0) tubes (476-atom unit cell). Further irradiation damage can produce atomic rearrangements leading to coalescence of nanotubes. (C and D) Two metastable states with a limited number of connections relaxed with MC from 1000°C up to -273°C in (10,10) and (17,0) nanotubes, respectively. (E and F) Two simulated annealing snapshots at 1000°C (unstable states) prior to coalescence, which form (20,20) and (34,0) nanotubes, respectively. These states are generated by increasing the number of connections along the tubes (zipping) in the configurations shown in (C) and (D).

into two sets of pentagon-heptagon pairs, on either sides of the tubes can cause the tubes to approach each other (in the range of 1000° to 800°C), establishing links through covalent sp<sup>3</sup> bonds (bond lengths close to that of diamond: 1.57 Å), which subsequently result in polymerized metastable states for both armchair and zig-zag tubes (Fig. 4, A and B). Therefore, it is possible that in our experiments intense electron irradiation at high temperature can continuously generate SWDs (15, 16) along the two tubes, producing a generalized polymerization scheme which may then follow coalescence. It is noteworthy that the nanotube polymerization is catalyzed by the local positive curvature of the pentagonal rings within the SWDs.

We also found that different topological types of defects connecting tubes (armchair and zig-zag) are metastable (strain energies of larger diameter tubes are lower than those of interconnected or smaller diameter tubes) when relaxed with MC from 1000° to -273°C (Fig. 4, C and D). When these connections increase in number along the tubes (zipping), unstable states are generated that quickly lead to coalescence at 1000°C (Fig. 4, E and F). All these calculations are in agreement with our experimental observations. The coalescence of two (10,10) tubes can lead to a (20,20) tube, although loss of atoms may lead to tubes of smaller diameter such as (18,18). The same might occur for two zig-zag (17,0) nanotubes coalescing to form a (34,0) or a smaller diameter tube.

We conclude that nanotube coalescence involves various phenomena that must simultaneously occur: (i) defect generation or the presence of reactive surface sites (such as vacancies, interstitials, dangling bonds, and SWDs); (ii) surface and atom reconstruction by chemical reactions (that could involve H termination) or

electron irradiation processes; and (iii) thermal annealing (zipping). It is highly likely that nanotubes contain ras-grown or irradiation-induced 5-7-7-5 (23) topological defects on their surface. These regions can be easily damaged, producing vacancies (dangling bonds), which will be the reactive sites that trigger coalescence; this process involves a zipping mechanism if the tubes possess the same chirality. In tubes with different chiralities, coalescence is unlikely because a large number of rearrangements of atoms need to take place along the tube lattice. However, local polymerization (topologically connected structures) results in such cases. Thermal processes and sufficient available kinetic energy (through annealing) are crucial both for coalescence and the formation of interconnections between nanotubes (polymerization). It has been experimentally observed that SWNTs heated above 2000°C in Ar (24) or He (25) atmospheres lead to either multiwalled carbon nanotubes (MWNTs) or coalesced SWNTs of larger diameters. Therefore, controlled irradiation or well-designed chemical reactions on C nanotube aggregates, followed by heat treatments, may generate fascinating interconnections. Alternatively, purely chemical-catalyzed coalescence of MWNTs (26) or SWNTs (27) of the same chirality may also be possible when hot, gaseous species such as B, Ni, or Co are present (unlike the case we discuss) within the system. Some predicted structures, such as Y-junctions, T-junctions, and nanotube joints, which are yet to be experimentally observed, may result from different coalescence sequences.

References and Notes

1. C. Yereztian, K. Hansen, F. Diederich, R. L. Whetten, *Nature* **359**, 44 (1992).
2. B. W. Smith, M. Monthoux, D. E. Luzzi, *Nature* **396**, 323 (1998).

3. J. Sloan *et al.*, *Chem. Phys. Lett.* **316**, 191 (2000)
4. S. L. Fang *et al.*, *J. Mater. Res.* **13**, 2405 (1998).
5. P. Nikolaev, A. Thess, A. G. Rinzler, D. T. Colbert, R. E. Smalley, *Chem. Phys. Lett.* **266**, 422 (1997).
6. A. J. Stone and D. J. Wales, *Chem. Phys. Lett.* **128**, 501 (1986).
7. R. Saito, G. Dresselhaus, M. S. Dresselhaus, *Chem. Phys. Lett.* **195**, 537 (1992).
8. M. Terrones and H. Terrones, *Full. Sci. Tech.* **4**, 517 (1996).
9. V. H. Crespi, M. L. Cohen, A. Rubio, *Phys. Rev. Lett.* **79**, 2093 (1997).
10. H. Terrones *et al.*, *Phys. Rev. Lett.* **84**, 1716 (2000).
11. L. A. Chernozatonskii, *Chem. Phys. Lett.* **297**, 257 (1998).
12. C. Journet *et al.*, *Nature* **388**, 756 (1997).
13. S. Goedecker and L. Colombo, *Phys. Rev. Lett.* **73**, 122 (1994).
14. C. H. Xu, C. Z. Wand, C. T. Chang, K. M. Ho, *J. Phys. Condens. Matter* **4**, 6047 (1992).
15. P. M. Ajayan, V. Ravikumar, J. C. Charlier, *Phys. Rev. Lett.* **81**, 1437 (1998).
16. F. Banhart, *Rep. Progr. Phys.* **62**, 1181 (1999).
17. ———, Ph. Redlich, P. M. Ajayan, *Chem. Phys. Lett.* **292**, 554 (1998).
18. D. H. Robertson, D. W. Brenner, J. D. Mintmire, *Phys. Rev. B* **45**, 12592 (1992).
19. N. Metropolis, A. Rosenbluth, M. Rosenbluth, A. Teller, E. Teller, *J. Chem. Phys.* **21**, 1087 (1953).
20. J. Tersoff, *Phys. Rev. Lett.* **61**, 2879 (1988).
21. A. Maiti, C. J. Brabec, C. Roland, J. Bernholc, *Phys. Rev. B* **52**, 14850 (1995).
22. H. Terrones, *Fullerene Sci. Technol.* **3**, 107 (1995).
23. M. B. Nardelli, B. I. Yakobson, J. Bernholc, *Phys. Rev. B* **57**, R4277 (1998).
24. S. Bonnamy and A. Oberlin, in *Graphite and Precursors*, P. Delhaes, Ed. (Gordon & Breach, Singapore, in press).
25. P. M. Ajayan, M. Terrones, Ph. Redlich, unpublished results.
26. X. Blase *et al.*, *Phys. Rev. Lett.* **83**, 5078 (1999).
27. A. Thess *et al.*, *Science* **273**, 483 (1996).
28. We are grateful to the Alexander von Humboldt Stiftung (M.T.), CONACYT-México grants 25237 and J31192U (H.T., M.T.), DGAPA-UNAM sabbatical scheme and grant 108199 (H.T.), and the Mexican Academy of Sciences (H.T.). J.C.C. acknowledges the National Fund for Scientific Research (FNRS) of Belgium and the Belgian Program on Interuniversity Attraction Poles on Reduced Dimensionality Systems (PAI4/10). P.M.A. acknowledges NSF for supporting his research through the CAREER program.

27 January 2000; accepted 4 April 2000